Thermodynamic and Structural Studies of Carbohydrate Binding by the Agrin-G3 Domain †

ARTICLE *in* BIOCHEMISTRY · SEPTEMBER 2007

Impact Factor: 3.02 · DOI: 10.1021/bi7006383 · Source: PubMed

3 AUTHORS, INCLUDING:

Andrei T Alexandrescu
University of Connecticut
74 PUBLICATIONS **2,215** CITATIONS

SEE PROFILE

Published in final edited form as:
Biochemistry. 2007 August 21; 46(33): 9541–9550.

Thermodynamic and Structural Studies of Carbohydrate Binding by the Agrin-G3 Domain†

Christine O. Sallum‡, **Richard A. Kammerer**§, and **Andrei T. Alexandrescu***,‡
Department of Molecular and Cell Biology, University of Connecticut, Storrs, Connecticut 06269-3125, and Wellcome Trust Centre for Cell-Matrix Research, Faculty of Life Sciences, University of Manchester, B.3011 Michael Smith Building, Oxford Road, Manchester M13 9PT, United Kingdom

Abstract

Agrin is a key heparan sulfate proteoglycan involved in the development and maintenance of synaptic junctions between nerves and muscles. Agrin's important functions include clustering acetylcholine receptors on the postsynaptic membranes of muscles and binding to the muscle protein α-dystroglycan through its glycan chains. ITC and NMR were used to study the interactions of the C-terminal domain, agrin-G3, with carbohydrates implicated in agrin's functions. Sialic acid caps the glycan chains of α-dystroglycan and occurs as a posttranslational modification on the muscle-specific kinase component of the agrin receptor. We found that agrin-G3 binds sialic acid in a Ca^{2+}-dependent manner. ITC data indicate that binding is exothermic and occurs with a 1:1 stoichiometry. NMR chemical shift changes map the sialic acid binding site to the loops that control the domain's acetylcholine receptor clustering activity. By contrast, the glycosaminoglycans heparin and heparan sulfate bind independently of Ca^{2+}. Binding is endothermic, and the binding site spans about 12 saccharide units. The binding site for heparin occupies a similar location but is distinct from that for sialic acid. NMR translational diffusion experiments show that agrin-G3 binds heparin with a 2:1 stoichiometry. Comparisons between the muscle (B0) and neuronal (B8) isoforms of the agrin domain showed very similar Ca^{2+} and carbohydrate binding properties. Our work identifies agrin-G3 as a functional analogue of the concanavalin A-type lectins, highlights functional similarities between agrin and laminin G domains, and provides mechanistic clues about the roles of carbohydrates in agrin's functions.

The heparan sulfate proteoglycan agrin is a critical component of neuromuscular junctions (NMJs)[1] (1). It has additional less well understood roles in the central nervous system (2,3), nonneural tissues (4), immunological synapses (5), and amyloid diseases (6,7). The agrin core protein consists of 22 domains. At the C-terminus are three globular G-domains separated by epidermal growth factor-like domains. The G-domains have a *β*-jellyroll folding motif structure (8) that belongs to the LNS superfamily, which includes domains from *l*aminin, *n*eurexin, and *s*teroid-hormone binding globule (9). Beyond the LNS family, the closest structural relatives are the pentraxins: serum amyloid P component and C-reactive protein. More distantly related folds include the concanavalin A-type lectins. Many of the proteins with folds structurally

†This work was supported by NSF Grant MB 0236316 to A.T.A. and NIH-NCRR funding for a 600 NMR instrument. R.A.K. is a Wellcome Trust Senior Research Fellow in Basic Biomedical Science.

* Corresponding author. Tel: (860) 486-4414. Fax: (860) 486-4331. E-mail: andrei@uconn.edu..
‡University of Connecticut.
§University of Manchester.

[1]Abbreviations: ACh, acetylcholine; AChR, acetylcholine receptor; α-DG, α-dystroglycan; G-domain, globular domain; GST, glutathione *S*-transferase; HSQC, heteronuclear single-quantum correlation; ITC, isothermal titration calorimetry; LG, laminin globular domain; LNS, *l*aminin, *n*eurexin, and steroid-hormone binding globule; MASC, myotube-associated specificity component; MuSK, muscle-specific kinase; NCAM, neural cell adhesion molecule; NMJ, neuromuscular junction; NMR, nuclear magnetic resonance; PFG-LED, pulse field gradient longitudinal encode–decode.

related to the agrin G-domains have carbohydrate binding functions, including the laminin G-domains, pentraxins, and C-type lectins. Carbohydrates have also been implicated in the functions of the agrin G-domains, prompting our efforts to characterize the thermodynamic and structural aspects of their binding.

One function of agrin is to form a structural bridge between the NMJ basal lamina and muscle (1,10). This interaction is mediated by the binding of the agrin G-domains to the glycan chains of α-dystroglycan (α-DG). Defects in the dystrophyn–glycoprotein complex, of which α-DG is a part, lead to the most common types of muscular dystrophy (11,12). Interactions between agrin and α-DG may also be important in synapse remodeling during the lifetime of the NMJ (1,13).

A second function of agrin for which the last globular domain G3 is necessary is to induce the aggregation of acetylcholine receptors (AChRs) on the postsynaptic plasma membranes of muscles, at sites juxtaposed to the nerve terminal (1). AChR aggregation is a hallmark of NMJ development (13,14), which is thought to be necessary for the timely and efficient communication between nerve and muscle via the neurotransmitter acetylcholine (ACh) (14). Recent data suggest that the agrin signal functions more generally, to maintain a dynamic equilibrium between the formation and dispersal of AChR clusters at mature NMJs. The neurotransmitter ACh disperses AChRs, while agrin is involved in the counteracting pathway to restore the receptor clusters (15,16). The AChR clustering activity requires the neural B^+/z^+ isoforms of agrin, which contain 8–19 residue sequence inserts between β-strands 2 and 3 of the G3 domain, derived from alternative mRNA splicing of the agrin gene. The insertless B0 isoform fails to aggregate AChR receptors.

Agrin does not induce aggregation of AChRs directly. Its signal is mediated through a muscle-specific kinase (MuSK), which in turn acts on a second messenger tyrosine kinase (17). Phosphorylation of the AChR β subunits triggers the aggregation of the receptors, together with additional proteins such as rapsyn (13,14). AChR clustering can be induced by C-terminal fragments of agrin as small as the 21 kDa agrin-G3 domain, albeit with a potency several hundred times lower than the full-length protein (1,18). A key question in understanding the mechanism by which agrin exerts its AChR clustering function is “what constitutes the receptor that leads to the activation of MuSK”? The agrin receptor is believed to be a complex, in which MuSK is the signaling component (17). Cross-linking experiments suggest that agrin binds (17) and activates MuSK in myotubes. It fails to do so, however, when expressed in other types of cells. These observations led to the hypothesis (17) of a coreceptor called myotube-associated specificity component (MASC). It has been suggested that MASC may be a carbohydrate, either displayed on the surfaces of myotubes or attached to agrin (19–21).

Here we describe an investigation of the binding of carbohydrates likely to play a role in agrin’s functions (Figure 1) to the agrin G3 domain: the domain that initiates the AChR clustering cascade. We show that, in the presence of Ca^{2+}, agrin binds sialic acid, a carbohydrate likely to be attached to the extracellular domains of MuSK and at the ends of the glycan chains of α-DG. Heparin and heparan sulfate, on the other hand, bind to the agrin-G3 domain in a Ca^{2+}-independent manner. The carbohydrate affinities investigated in this work are similar for the B0 and B8 isoforms of agrin-G3, indicating that the B-inserts required for agrin’s AChR clustering function are not determinants of carbohydrate binding, in spite of the fact that the carbohydrate binding sites on the agrin-G3 domain are close to the B^+/z^+ insert loops.

EXPERIMENTAL PROCEDURES

Materials

Sialic acid (*N*-acetylneuraminic acid IV-S, catalog no. A0812), Gal(β1,3)GalNAc (A0167), Gal(β1,4)-GlcNAc (A7791), heparin (MW 4–6 kDa, sodium salt, H8537), and $CaCl_2$ (C3881) were all from Sigma-Aldrich (St. Louis, MO). Heparin I-S disaccharide [α-4-deoxy-L-*threo*-hex-4-enopyranosyluronic acid 2-sulfate (1→4)-*N*-sulfo-D-glucosamine 6-sulfate, H1001] was from V-labs (Covington, LA). Heparan sulfate (sodium salt from porcine intestinal mucosa, MW 15 ± 2 kDa, HO 03102) was from Celsus Laboratories (Cincinnati, OH).

Expression and Purification of Agrin-G3(B0) and -G3-(B8) Domains

The agrin-G3(B0) domain comprises residues Glu1752–Lys1944 of the chicken agrin protein (Swissprot: P31696, B0 splice form). The neural B8 isoform contains the specific eight-residue splice insert HLSNEIPA following Ser1782. The 21 kDa agrin-G3 fragment used for the present work is based on a construct (8,22) that has the N-terminal domain boundary extended by 10 residues compared to earlier fragments (18,20,23,24). The newer construct is more stable to precipitation, a factor that was critical in determining the NMR structure of the domain. Genes encoding the agrin-G3 domains were incorporated into the pGSTHis vector, a derivative of pGEX-1 (Amersham Biosciences) that encodes a glutathione *S*-transferase (GST) carrier protein, followed by a His_6 tag, a thrombin cleavage site, and the agrin-G3 domain of interest (25). Unlabeled domains were expressed in BL21 *Escherichia coli* cells using the overnight express autoinduction system 1 (Novagen), supplemented with 50 μg/mL ampicillin (26). ^{15}N-Labeled G3 domains for NMR studies were expressed in MOPS minimal media plus the autoinduction system, with buffer 2 replaced by 1 g of [^{15}N]ammonium chloride/L of culture. Following expression, cells were harvested by centrifugation at 2100 rpm and a temperature of 4 °C and resuspended in 20 mM phosphate and 150 mM NaCl, pH 7.3 (PBS), containing 20 mM EDTA and 1 tablet of Complete protease inhibitor (Roche) per 50 mL of buffer. The cell suspension was sonicated at 50% power for 3 min using six pulses of 30 s. Cell debris was removed by centrifugation for 15 min at 10900 rpm and 4 °C. The supernatant was loaded onto a 100 mL glutathione–Sepharose 4 fast-flow affinity column (Amersham Biosciences) and washed with PBS. The G3 domain was then cleaved from the GST carrier on-column for 16 h using bovine thrombin (Amersham Biosciences) and eluted with PBS. Thrombin was removed by incubation at room temperature for 30 min with benzamidine–Sepharose (Amersham Biosciences). Agrin-G3 domain concentrations were determined using a ε_{280} extinction coefficient of 24750 M^{-1} cm^{-1}.

To prepare Ca^{2+}-free samples, the domain was incubated for 30 min at 4 °C in 10 mM imidazole buffer (pH 6.2) containing 10 mM EDTA. To remove the EDTA, the samples were dialyzed at 4 °C overnight against the imidazole buffer prepared with MilliQ water.

ITC Data Acquisition and Analysis

Before use, samples and buffers were passed through 0.22 μm syringe filters. Agrin-G3 samples were loaded into the well of a VP-ITC microcalorimeter (MicroCal). Ligand was injected in at least 25 increments to the desired final molar ratio, using an injection rate of 1 μL/2 s and an equilibration delay of 6 min between injections. For the calcium binding experiments, samples contained 60 μM agrin-G3(B0) or 48 μM agrin-G3(B8). For the sialic acid binding experiments, protein concentrations were 310 μM agrin-G3(B0) or 160 μM agrin-G3(B8). For the heparin and heparan sulfate binding experiments, samples had 50 μM protein. The calcium, heparin, and heparan sulfate binding experiments were done on Ca^{2+}-free agrin samples. For the sialic acid binding experiments, both the sialic acid and agrin-G3 solutions were maintained at 17 mM $CaCl_2$. This Ca^{2+} concentration was determined to be saturating for both the protein and sugar. In separate experiments ligands were injected into 10 mM imidazole buffer (pH 6.2)

without the protein, and the data were used for ligand-to-buffer background subtraction. ITC data were analyzed with Origin 5.0 software and with the curve-fitting program Igor Pro (Wavemetrics, Lake Oswego, OR). All experiments were done at 25 °C.

NMR Spectroscopy

Except where indicated, NMR experiments were done on a Varian 600 MHz instrument equipped with a cryoprobe. All NMR data were acquired at a temperature of 25 °C, and all agrin-G3 samples were in 10 mM imidazole buffer, pH 6.2. To monitor binding, $^{1}H–^{15}N$ HSQC experiments were recorded with spectral widths of 8000 ×1700 Hz digitized into matrices of 2048 ×128 complex points in the $^{1}H \times ^{15}N$ dimensions. NMR assignments for agrin-G3 were published previously (22). Sialic acid NMR titrations used 0.45 mM agrin-G3(B0) and sialic acid concentrations of 0, 0.05, 0.14, 0.27, 0.90, 2.25, and 4.5 mM. Heparin NMR titrations used 0.15 mM agrin-G3-(B0) and heparin concentrations of 0, 0.05, 0.1, 0.2, 0.4, 1.0 and 2.0 mM.

Pulse Field Gradient Diffusion Experiments

One-dimensional PFG-LED NMR experiments (27) were performed on a Bruker 500 MHz spectrometer using samples of 0.5 Mm agrin-G3(B0) in a 99.96% D_2O solution of 5 mM $CaCl_2$ and 10 mM imidazole, pH 6.2. Although binding of B0 to heparin is independent of Ca^{2+}, 5 mM $CaCl_2$ was included to stabilize protein solutions against aggregation during the ~1 day PFG-LED experiments (22,25). Samples also included 1 μL of 1% dioxane, which was used as a diffusion reference standard. To look at the effects of heparin binding, samples were prepared the same way except including 4 mg of heparin/300 μL of protein solution (~2.6 mM heparin).

RESULTS

Thermodynamics of Ca^{2+} Binding

Binding of Ca^{2+} to agrin-G3 has been studied previously by NMR (22,25) and CD (28). NMR gave K_d values for Ca^{2+} of 600 μM for B0 and 100 μM for B8 (8). In contrast, CD experiments indicated a much weaker K_d of 10 mM for the neural B8 domain and pointed to a large conformational change accompanying Ca^{2+} binding by the B8 variant but not B0 (28). NMR data showed no evidence for a conformational transition but indicated a significant reduction in the mobility of the loops surrounding the Ca^{2+} binding site in the bound states of both B0 and B8 (8).

We further characterized Ca^{2+} binding by ITC (Table 1). The dissociation constants of 260 μM for B0 and 500 μM for B8 that we obtained by ITC are in reasonable agreement with those from NMR. The change in enthalpy from ITC is similar for B0 and B8 and indicates that Ca^{2+} binding is exothermic. The change in entropy is unfavorable, a facet probably related to the “freezing out” of conformational dynamics in the Ca^{2+}-bound state detected by ^{15}N NMR relaxation experiments (25).

Binding of Sialic Acid

We next looked at binding of the agrin-G3 domain to *N*-acetylneuraminic acid (Neu5Ac), the simplest sialic acid (29). Although the unique role of neural agrin isoforms is to stimulate AChR clustering, the likely function of the muscle-derived B0 isoform is to bind α-DG at the NMJ synapse (18,23). Agrin binds α-DG through its glycan chains, which in myotubes and in skeletal muscle are capped by sialic acid (30,31). Moreover, sialic acid is found on at least two other molecules that interact with agrin: NCAM (32) and MuSK (33). Finally, considerable evidence supports a role for sialic acid as a modulator of agrin’s AChR clustering activity.

Neuraminidase, an enzyme that removes terminal sialic acid residues, activates AChR clustering. Conversely, free sialic acid inhibits clustering at millimolar concentrations (20, 34–36).

Sialic acid itself binds Ca^{2+} weakly, with a K_d of 8 mM (37). To ensure that we were measuring the thermodynamics of sialic acid binding to agrin-G3, rather than heat changes associated with Ca^{2+} binding to sialic acid, we did the experiments at a fixed Ca^{2+} concentration of 17 mM. We determined by ITC that a 17 mM concentration of Ca^{2+} is saturating for both the G3 domain and sialic acid (not shown). Representative ITC data are shown in Figure 2A, and the thermodynamic parameters characterizing binding to B0 and B8 are summarized in Table 1. Sialic acid binds the agrin-G3 domain with a 1:1 stoichiometry and with a weak dissociation constant in the 1 mM range. The ITC parameters for the B0 and B8 isoforms are similar, which leads us to conclude that the insert site in the neural B8 isoform has a negligible impact on affinity for sialic acid. Importantly, we did not observe binding of sialic acid in the absence of Ca^{2+}, indicating that the metal ion is required. NMR signals of the agrin-G3 domain showed gradual changes in chemical shifts as the concentration of sialic acid increased. The free and sialic acid bound states of agrin-G3 (Figure 3A) are thus in fast exchange on the NMR time scale, consistent with the weak binding (K_d ~ 1 mM) observed by ITC.

Heparin and Heparan Sulfate Binding

Heparin is a highly sulfated glycosaminoglycan that occurs mainly in mast cells but is commonly used as a model for the glycan chains of heparan sulfate proteoglycans found in the extracellular matrix (7). In addition to heparin we also characterized the binding of agrin-G3 to heparan sulfate, since the two glycosaminoglycans do not always give analogous results (38). The latter is more relevant to the heparan sulfate proteoglycans agrin would encounter in the extracellular matrix, and agrin itself is a heparan sulfate proteoglycan.

Binding of heparin leads to initial differential decreases of cross-peaks in $^{1}H–^{15}N$ HSQC spectra of agrin-G3, followed by attenuation of most resonances from the protein at saturating concentrations of the glycosaminoglycan (Figure 3B). As described below, this is due to a combination of the free and heparin-bound forms of the agrin-G3 domain being in intermediate exchange and the large size of the agrin–heparin complex. ITC data for heparin binding are shown in Figure 2B, and thermodynamic parameters for heparin and heparan sulfate binding are summarized in Table 1. The ITC experiments were done in the absence of Ca^{2+}, using agrin-G3 pretreated with EDTA to remove metal ions. In contrast to sialic acid, Ca^{2+} is not needed for binding of heparin or heparan sulfate to the agrin-G3 domain. Binding of heparin and heparan sulfate is endothermic (39), a feature that appears to have been previously observed in ITC of other heparin binding proteins (40–42). The K_d values for both heparin and heparan sulfate are in the 10 μM range (Table 1), consistent with intermediate exchange on the NMR time scale. There is little difference in binding affinity, in stoichiometry, or in the thermodynamics of binding between the B0 and B8 isoforms of agrin-G3 (Table 1).

NMR failed to detect binding of the most heavily sulfated I-S disaccharide unit of heparin (43) even when the carbohydrate was held at a 10 mM concentration, a large excess over the protein (not shown). This suggests that the recognition epitope for agrin is larger than a disaccharide. The low MW heparin fraction we used had a MW range of 5 ± 1 kDa. The molecular mass of an average glycosaminoglycan disaccharide unit is ~640 Da, so the average degree of polymerization (dp) for the heparin employed in this work was ~16 saccharides. The heparan sulfate fraction had a larger mean MW of 15 ± 2 kDa, corresponding to an average dp of 48 saccharides. The ITC experiments revealed an n of ~0.8 for heparin titrated into agrin-G3. This indicates that ~1.2 agrin-G3 molecules are bound for every dp = 16 heparin chain. With heparan sulfate, which had average glycosaminoglycan chains three times as long (dp = 48), the n-value of ~0.25 was correspondingly smaller, suggesting that on average ~4 agrin

molecules bound each of the longer heparan sulfate chains. The *n*-values obtained from ITC therefore indicate a binding site of ~12 saccharide monomers, for both heparin and heparan sulfate.

Agrin-G3 Fails To Bind to Carbohydrate Moieties of the CT Antigen in Solution

The disaccharides Gal(*β*1,3)GalNAc and Gal(*β*1,4)GlcNAc are subunits of the CT antigen, a carbohydrate antigen specifically expressed at the NMJ (19,20) and proposed as a candidate for the MASC component of the agrin receptor (20). Both sugars bound MuSK, in an assay where the disaccharides were immobilized on a resin, and MuSK was detected with antibodies to a FLAG tag (20). The neural B8 isoform of agrin-G3 was reported to bind to Gal(*β*1,3) GalNAc but not to Gal(*β*1,4)GlcNAc based on the same immobilized assay (20), whereas the inactive B0 isoform failed to bind either disaccharide. We did not detect binding of Gal(*β*1,3) GalNAc or Gal(*β*1,4)GlcNAc to either the B0 or B8 isoforms of the agrin-G3 domain by NMR, even at disaccharide concentrations as high as 7.5 mM, a 50-fold excess over the 0.15 mM agrin-G3 domain. The experiments were done for the G3 domain in the presence of 5 mM $CaCl_2$, since Ca^{2+} could conceivably be required for binding. The discrepancy between the solid-phase assay and NMR results may be due to the disaccharides having been immobilized on a solid-phase support in the former study (20).

Structural Mapping of the Sialic Acid Binding Site

The residues that experience the largest chemical shift differences between the free and sialic acid bound forms of the protein (Figure 4A) map to the interaction interface loops in the NMR structure of the agrin-G3 domain (Figure 4C). These include residues from loop L2–3 (Asn29, Ala30, Ser34, Glu35, Ala37), loop L4–5 (Gly62, Leu63, Asp67, Tyr68), loop L6–7 (Asp83, Gly85), loop L10–11 (Gly131, Ala132, Asp136, Thr137, Gly139, Ala140), and His153 in the *ω* loop outside of the interaction interface. Roughly the same regions of the structure show the largest perturbations when Ca^{2+} binds (8), an observation that further supports an obligatory role for the metal in sialic acid binding. Chemical shift changes when sialic acid binds are very similar for the B0 and B8 isoforms (not shown), which together with the ITC data indicate that the eight-residue B8 insert has little bearing on sialic acid binding.

Structural Mapping of the Heparin Binding Site

In order to characterize heparin binding, we determined rates of cross-peak decays in $^{1}H–^{15}N$ HSQC spectra of agrin-G3 as a function of increasing glycosaminoglycan concentration (44, 45). In contrast to the chemical shift changes with sialic acid, heparin affects cross-peaks throughout the $^{1}H–^{15}N$ HSQC spectrum of agrin-G3 (Figure 4B). Nevertheless, the residues that experience the largest decay constants, the sites that are most sensitive to heparin concentration, map to a similar region of the structure as the residues most affected by sialic acid (Figure 4D). The $^{1}H–^{15}N$ HSQC peaks with the largest perturbations when heparin binds are from the two loops L4–5 (Gly62, Arg65, Ile69) and L10–11 (Gly131, Gly139) that provide ligands for Ca^{2+} and the hairpin loops connecting strands *β*8–*β*9 (Tyr108, Val110, Glu113, Val118) and *β*12-*β*13 (Asp173, Arg174) in the convex *β*-sheet (Figure 4D). Three additional residues outside the interaction interface also show large decay constants on heparin binding: Thr94, Ala122, and Leu179 in the short α-helix following *β*-strand 13. Two of the loops strongly affected by sialic acid, the Ca^{2+}-ligand loop L6–7 and the insert-bearing loop L2–3, are relatively unperturbed by heparin binding. The NMR changes accompanying heparin binding are in agreement with a mutagenesis study of a homologous LG5 domains from laminin, where mutations in the *β*8–*β*9 and *β*12–*β*13 hairpins of the convex *β*-sheet had the largest impact on heparin binding (46). The mutagenesis study identified a secondary heparin binding site in laminin domain LG4 that included two residues from the beginning of loop L10–11, which is also perturbed by heparin in agrin (Figure 4B,D).

Although NMR signals from the interface loops are affected by both sialic acid and heparin, indicating partially overlapping binding sites, there are important differences between the two ligands. The perturbations of residues in the convex β-sheet are only seen with heparin binding, and two of the loops L2–3 and L6–7 involved in sialic acid binding appear not to be strongly affected by heparin. Most notably, Ca^{2+} is required for sialic acid binding but not for heparin. We therefore conclude that the two binding sites are distinct.

Oligomerization State of Heparin-Bound Agrin

Differential line broadening is observed in $^{1}H–^{15}N$ HSQC spectra of the G3 domain upon addition of heparin. At saturating concentrations of heparin, most of the agrin-G3 cross-peaks have undergone significant decreases in intensity (Figure 3B). Line broadening could be due to exchange processes on the microsecond to millisecond intermediate time scale, due to agrin-G3 binding heparin as a large molecular weight oligomer with short T_2 transverse relaxation times, or both mechanisms.

To test for the molecular size of the complex, we conducted 1D PFG-LED (27) experiments on the agrin-G3 domain in the absence and presence of heparin (Figure 5). In the 1D PFG-LED experiments, NMR signals decay with increasing gradient strength. The decay rate is proportional to the molecular diffusion coefficient (d_p). The hydrated radius of the protein $R_{h,p}$ can be obtained from the measured diffusion coefficients of the protein, the internal standard 1,4-dioxane (d_d), and the known hydrated radius ($R_{h,d}$) of dioxane according to the equation $R_{h,p} = (d_d/d_p)R_{h,d}$ (47).

Using this method we obtained an R_h value of 21.2 Å for the agrin-G3 domain alone (Figure 5A) and 29.0 Å for the agrin-G3 domain in the presence of heparin (Figure 5B). The R_h for the protein alone is consistent with a prediction of 21.9 Å for a 195-residue domain, obtained using the empirically derived formula $R_h = 4.75N^{0.29}$, where N is the number of residues (47). For the domain in the presence of heparin, the apparent R_h of 29 Å is consistent with a complex about 2.5 times the size of the agrin-G3 monomer (47). This would roughly correspond to two agrin domains (21 kDa each) and one heparin molecule (~5 kDa). We therefore conclude that the agrin-G3 domain binds heparin with a 2:1 stoichiometry.

DISCUSSION

The classical biology approaches used to identify the molecular components of neuromuscular junctions (1,11,13,14,17,21) have recently begun to be complemented by biophysical and structural studies which provide mechanistic information about molecular function (25,46, 48–53). In the case of the agrin-G3 domain, it has been established that the domain adopts an LNS β-jellyroll fold structure (8), that the insert loops required for AChR clustering activity occur in a dynamically flexible region of the protein between strands β2 and β3 (8), and that the agrin-G3 domain binds Ca^{2+} (22,28) which reduces but does not eliminate the mobility of the surface loops that mediate the domain's activities (8). In the present work we have used structural and biophysical methods to examine the binding of the agrin-G3 domain to carbohydrates that are likely to play key roles in agrin's functions.

Sialic Acid Binding

Sialic acid binds the agrin-G3 domain weakly with a K_d in the ~1 mM range (Table 1). Affinity could be enhanced considerably, however, in the full-length proteoglycan where multiple agrin G-domains participate cooperatively in binding or when additional cofactors participate in complex formation. In vivo, both α-DG binding and MuSK activation require multiple G-domains for optimum efficiency (54). Moreover, while we studied binding to a single sialic acid monomer, the physiologically relevant interactions may involve sialic acid moieties as

part of more complex molecules or polymers with higher avidity for agrin. The experiments with the isolated G3 domain establish that sialic acid binds with a 1:1 stoichiometry and that binding requires Ca^{2+} and the location of the sialic acid binding site in the structure. The binding site based on NMR chemical shift perturbation data involves the three calcium binding loops L4–5, L6–7, and L10–11 from the "interaction interface" region of the β-sandwich structure and loop L23 which in neural isoforms of agrin has the B^+ sequence inserts. The location of the sialic acid binding site and the Ca^{2+} requirement for binding argue for an important role for the carbohydrate since Ca^{2+} is needed for the AChR clustering activity (28,55) as well as for binding of agrin to α-DG (56).

The presence of B^+ inserts has little effect on the binding of the G3 domain to sialic acid. It is of interest to note in this regard that a recent mutagenesis study found that of the eight residues in the B8 insert only three are critically important for activating MuSK (57). Presumably, this Asp-Glu-Ile triplet in the B8 insert sequence forms the key defining interactions that are necessary to activate the muscle-specific kinase.

Possible Roles for Sialic Acid in Interactions between Agrin and MuSK

There is considerable circumstantial evidence supporting a role for sialic acid in agrin's AChR clustering function. Removal of cell surface sialic acid from C2 myotubes with neuraminidase induces MuSK phosphorylation and simulates AChR clustering as much as agrin, but in a mechanism that is apparently independent of either agrin or laminin (20,34–36). By contrast, millimolar concentrations of free sialic acid, similar to the concentrations used in this study, inhibit both MuSK phosphorylation and AChR clustering (32). It has been proposed that sialic acid affects AChR clustering downstream of MuSK. This conclusion, however, was based on colocalization of agrin with AChRs at sialic acid concentrations that inhibited the majority of AChR clusters. The clusters that survived may be those that escaped sialic acid inhibition (32). The observation that sialic acid binds to the G3 domain in a Ca^{2+}-dependent manner suggests a simpler alternative mechanism, in which the carbohydrate interferes directly with the interactions between agrin and MuSK.

MuSK, the critical component of the receptor that transduces agrin's AChR aggregating activity, appears to be sialylated itself since neuraminidase treatment decreases the apparent size of the kinase on immunoblot gels (36) and since lectins specific to sialic acid bind to glycosylated MuSK (33). Sialic acid is thought to be attached to MuSK through two conserved N-linked glycosylation sites, one of which is on the second of three extracellular immunoglobulin domains that are involved in agrin binding. The agrin-G3 domain could bind sialic acid on MuSK, unmasking kinase activity by relieving the inhibition caused by the carbohydrate. Alternatively, a molecular analogue of sialic acid may represent a functionally relevant binding partner of the agrin-G3 domain such as MASC. While identifying sialic acid as a binding partner for the agrin-G3 domain, we found that the Gal(β1,3)GalNAc disaccharide component of the CT antigen which was previously suggested as a candidate for MASC (20) does not bind to the neural B8 variant of the agrin-G3 domain in solution, although it may do so when presented in an immobilized form.

Additional Roles for Sialic Acid in Agrin Function

Sialic acid caps the glycan chains of α-DG and could be involved in the binding of agrin to α-DG, in analogy to the roles of the G-domains in laminin (30). In contrast to the neural isoforms, the agrin B0 isoform is inactive in AChR clustering, and its primary role at the NMJ is to form part of the link between the basal lamina and α-DG emanating from the muscle (1). In addition to α-DG, sialic acid moieties also occur in other potential agrin interaction partners such as the neural cell adhesion molecule (NCAM) (32) and in GM1 gangliosides, sphingolipids found in

high concentrations at synaptic membranes where they have roles in synaptic transmission (45).

Glycosaminoglycan Binding

We have shown that both heparin and heparan sulfate bind to the agrin-G3 domain with K_d values in the ~10 μM range (Table 1). Binding is independent of Ca^{2+}, and we find that the agrin-G3 domain binds the low MW heparin (4–6 kDa) used in this study with a 2:1 stoichiometry, which may reflect the native preference for binding a pair of agrin G-domains. The binding site recognized by agrin corresponds to ~12 saccharide monomers for both heparin and heparan sulfate. The heparin binding site partially overlaps but shows important differences from that for sialic acid (Figure 4C,D). The most compelling evidence for distinct binding sites is that while sialic acid requires Ca^{2+} for binding, heparin does not. These results are similar to observations for the homologous laminin G-domains, where Ca^{2+} was shown to be required for binding to α-DG but not for binding to heparin (46,58). Heparin was previously reported to bind only to variants of the G2 domain that contained the four-residue A-splice insert sequence KSRK (18,23,24). The agrin-G3 domain was not retained on heparin affinity columns and was thought not to bind. The origins of the apparent discrepancies with earlier results are unclear. The G2 domain may have a much higher affinity for heparin than the G3 domain, although no quantitative binding affinity data are available from the heparin column experiments (18,23,24).

The structural mapping of the heparin binding site in agrin qualitatively agrees with results from a mutational analysis of heparin binding to the laminin G5 domain (46). The mutagenesis study found that the sites with the greatest effect on heparin affinity are located in loops L2–3, L8–9, and L12–13 of the LG5 domain (46,53). In agrin-G3, heparin strongly perturbs NMR signals from loops L8–9 and L12–13. We did not see an effect on loop L2–3, but resonances from this loop are weak because of NMR exchange broadening. The NMR results point to a more extended binding site that also includes loop L4–5. The interaction interface loops of agrin-G3 are more negatively charged than those in the laminin LG5 domain (Figure 4 of ref 25), which probably accounts for the weaker affinity of agrin-G3 for negatively charged substrates like heparin and α-DG. Nevertheless, in spite of the weak sequence homology of only 20% between the LG5 and agrin-G3 domains, and the unfavorable negatively charged surface in the agrin-G3 domain, some of the residues that have been shown by mutagenesis (46,53) to be important for binding of heparin to LG5 (Lys3028 and Lys3030 in loop L8–9, Lys3095 in loop L12–13) appear to have analogues in agrin-G3 (Arg109 and Arg112 in L8–9, Arg174 in L12–13) that are perturbed by heparin binding based on the NMR data (Figure 4B,D). These residues may in part account for the ability of agrin-G3 to bind heparin.

Functional Implications of Glycosaminoglycan Binding

While heparin is a model for the glycan chains of α-DG, there are important differences in the interactions of the two molecules with agrin. First, binding of α-DG to agrin is Ca^{2+}-dependent, while heparin binding is not (18,23). This is consistent with the Ca^{2+}-independent binding of heparin to the agrin-G3 domain observed in this study. Second, the presence of the B^+ inserts in agrin greatly diminishes the affinity for α-DG but not for heparin (18,23). Consistently, we found no change in affinity for heparin or heparan sulfate between the B0 and B8 isoforms of the G3 domain (Table 1). Binding to α-DG must involve additional interactions compared to heparin or heparan sulfate that discriminate between the B0 and B8 isoforms.

Because the properties of heparin and heparan sulfate are not always equivalent, we decided to test for the binding of heparan sulfate to the G3 domain, since this glycosaminoglycan is more relevant to the extracellular matrix (38). Heparan sulfate binds the G3 domain with an affinity similar to that of heparin (Table 1). Agrin itself is a heparan sulfate proteoglycan so

the binding of the agrin-G3 domain to heparan sulfate raises the possibility that the domain could interact with its own glycan chains in the N-terminal half of the molecule (8). Yet another possibility is that agrin-G3–heparan sulfate interaction could cross-link proteoglycan molecules. Agrin and other heparan sulfate proteoglycans are found attached to Alzheimer's amyloid deposits through their heparan sulfate chains (6,7,59), and intermolecular cross-linking could conceivably aggravate amyloid deposition.

Acknowledgements

We are greatly indebted to Prof. James Cole for advice with ITC experiments and suggestions regarding the manuscript. We thank Bill Matousek and Martha Morton for help with the PFG diffusion experiments and Sid Tansey and Mani Seetharaman for technical assistance.

References

1. Bezakova G, Ruegg MA. New insights into the roles of agrin. Nat Rev Mol Cell Biol 2003;4:295–308. [PubMed: 12671652]
2. Kroger S, Schroder JE. Agrin in the developing CNS: new roles for a synapse organizer. News Physiol Sci 2002;17:207–212. [PubMed: 12270958]
3. Burgess RW, Dickman DK, Nunez L, Glass DJ, Sanes JR. Mapping sites responsible for interactions of agrin with neurons. J Neurochem 2002;83:271–284. [PubMed: 12423238]
4. McMahan UJ, Horton SE, Werle MJ, Honig LS, Kroger S, Ruegg MA, Escher G. Agrin isoforms and their role in synaptogenesis. Curr Opin Cell Biol 1992;4:869–874. [PubMed: 1329871]
5. Khan AA, Bose C, Yam LS, Soloski MJ, Rupp F. Physiological regulation of the immunological synapse by agrin. Science 2001;292:1681–1686. [PubMed: 11349136]
6. Donahue JE, Berzin TM, Rafii MS, Glass DJ, Yancopoulos GD, Fallon JR, Stopa EG. Agrin in Alzheimer's disease: altered solubility and abnormal distribution within microvasculature and brain parenchyma. Proc Natl Acad Sci USA 1999;96:6468–6472. [PubMed: 10339611]
7. Alexandrescu AT. Amyloid accomplices and enforcers. Protein Sci 2005;14:1–12. [PubMed: 15576561]
8. Stetefeld J, Alexandrescu AT, Maciejewski MW, Jenny M, Rathgeb-Szabo K, Schulthess T, Landwehr R, Frank S, Ruegg MA, Kammerer RA. Modulation of agrin function by alternative splicing and Ca^{2+} binding. Structure (Cambridge) 2004;12:503–515.
9. Rudenko G, Hohenester E, Muller YA. LG/LNS domains: multiple functions–one business end? Trends Biochem Sci 2001;26:363–368. [PubMed: 11406409]
10. Moll J, Barzaghi P, Lin S, Bezakova G, Lochmuller H, Engvall E, Muller U, Ruegg MA. An agrin minigene rescues dystrophic symptoms in a mouse model for congenital muscular dystrophy. Nature 2001;413:302–307. [PubMed: 11565031]
11. Durbeej M, Campbell KP. Muscular dystrophies involving the dystrophin-glycoprotein complex: an overview of current mouse models. Curr Opin Genet Dev 2002;12:349–361. [PubMed: 12076680]
12. Martin PT, Freeze HH. Glycobiology of neuromuscular disorders. Glycobiology 2003;13:67R–75R.
13. Sanes JR, Lichtman JW. Induction, assembly, maturation and maintenance of a postsynaptic apparatus. Nat Rev Neurosci 2001;2:791–805. [PubMed: 11715056]
14. Sanes JR, Lichtman JW. Development of the vertebrate neuromuscular junction. Annu Rev Neurosci 1999;22:389–442. [PubMed: 10202544]
15. Yang X, Arber S, William C, Li L, Tanabe Y, Jessell TM, Birchmeier C, Burden SJ. Patterning of muscle acetylcholine receptor gene expression in the absence of motor innervation. Neuron 2001;30:399–410. [PubMed: 11395002]
16. Kummer TT, Misgeld T, Sanes JR. Assembly of the postsynaptic membrane at the neuromuscular junction: paradigm lost. Curr Opin Neurobiol 2006;16:74–82. [PubMed: 16386415]
17. Glass DJ, Bowen DC, Stitt TN, Radziejewski C, Bruno J, Ryan TE, Gies DR, Shah S, Mattsson K, Burden SJ, DiStefano PS, Valenzuela DM, DeChiara TM, Yancopoulos GD. Agrin acts via a MuSK receptor complex. Cell 1996;85:513–523. [PubMed: 8653787]

18. Gesemann M, Cavalli V, Denzer AJ, Brancaccio A, Schumacher B, Ruegg MA. Alternative splicing of agrin alters its binding to heparin, dystroglycan, and the putative agrin receptor. Neuron 1996;16:755–767. [PubMed: 8607994]
19. Xia B, Martin PT. Modulation of agrin binding and activity by the CT and related carbohydrate antigens. Mol Cell Neurosci 2002;19:539–551. [PubMed: 11988021]
20. Parkhomovskiy N, Kammesheidt A, Martin PT. N-acetyllactosamine and the CT carbohydrate antigen mediate agrin-dependent activation of MuSK and acetylcholine receptor clustering in skeletal muscle. Mol Cell Neurosci 2000;15:380–397. [PubMed: 10845774]
21. Martin PT. Glycobiology of the synapse. Glycobiology 2002;12:1R–7R. [PubMed: 11825880]
22. Alexandrescu AT, Maciejewski MW, Ruegg MA, Engel J, Kammerer RA. ^{1}H, ^{13}C and ^{15}N backbone assignments for the C-terminal globular domain of agrin. J Biomol NMR 2001;20:295–296. [PubMed: 11519755]
23. Campanelli JT, Gayer GG, Scheller RH. Alternative RNA splicing that determines agrin activity regulates binding to heparin and alpha-dystroglycan. Development 1996;122:1663–1672. [PubMed: 8625852]
24. Cornish T, Chi J, Johnson S, Lu Y, Campanelli JT. Globular domains of agrin are functional units that collaborate to induce acetylcholine receptor clustering. J Cell Sci 1999;112(Part 8):1213–1223. [PubMed: 10085256]
25. Stetefeld J, Jenny M, Schulthess T, Landwehr R, Schumacher B, Frank S, Ruegg MA, Engel J, Kammerer RA. The laminin-binding domain of agrin is structurally related to N-TIMP-1. Nat Struct Biol 2001;8:705–709. [PubMed: 11473262]
26. Studier FW. Protein production by auto-induction in high density shaking cultures. Protein Expression Purif 2005;41:207–234.
27. Altieri AS, Hinton DP, Byrd RA. Association of biomolecular systems *via* pulsed field gradient NMR self-diffusion measurements. J Am Chem Soc 1995;117:7566–7567.
28. Tseng CN, Zhang L, Cascio M, Wang ZZ. Calcium plays a critical role in determining the acetylcholine receptor-clustering activities of alternatively spliced isoforms of agrin. J Biol Chem 2003;278:17236–17245. [PubMed: 12621054]
29. Angata T, Varki A. Chemical diversity in the sialic acids and related alpha-keto acids: an evolutionary perspective. Chem Rev 2002;102:439–469. [PubMed: 11841250]
30. Chiba A, Matsumura K, Yamada H, Inazu T, Shimizu T, Kusunoki S, Kanazawa I, Kobata A, Endo T. Structures of sialylated O-linked oligosaccharides of bovine peripheral nerve alpha-dystroglycan. The role of a novel O-mannosyl-type oligosaccharide in the binding of alpha-dystroglycan with laminin. J Biol Chem 1997;272:2156–2162. [PubMed: 8999917]
31. Ervasti JM, Burwell AL, Geissler AL. Tissue-specific heterogeneity in alpha-dystroglycan sialoglycosylation. Skeletal muscle alpha-dystroglycan is a latent receptor for *Vicia villosa* agglutinin b4 masked by sialic acid modification. J Biol Chem 1997;272:22315–22321. [PubMed: 9268382]
32. Grow WA, Gordon H. Sialic acid inhibits agrin signaling in C2 myotubes. Cell Tissue Res 2000;299:273–279. [PubMed: 10741468]
33. Watty A, Burden SJ. MuSK glycosylation restrains MuSK activation and acetylcholine receptor clustering. J Biol Chem 2002;277:50457–50462. [PubMed: 12399462]
34. Parkhomovskiy N, Martin PT. Alpha-galactosidase stimulates acetylcholine receptor aggregation in skeletal muscle cells via PNA-binding carbohydrates. Biochem Biophys Res Commun 2000;270:899–902. [PubMed: 10772922]
35. Martin PT, Sanes JR. Role for a synapse-specific carbohydrate in agrin-induced clustering of acetylcholine receptors. Neuron 1995;14:743–754. [PubMed: 7718237]
36. Grow WA, Ferns M, Gordon H. Agrin-independent activation of the agrin signal transduction pathway. J Neurobiol 1999;40:356–365. [PubMed: 10440735]
37. Jaques LW, Brown EB, Barrett JM, Brey WSJWW Jr. Sialic acid. A calcium-binding carbohydrate. J Biol Chem 1977;252:4533–4538. [PubMed: 873904]
38. Kiselevsky R, Szarek WA, Ancsin J, Bhat S, Li Z, Marone S. Novel glycosaminoglycan precursors as anti-amyloid agents, Part III. J Mol Neurosci 2003;20:291–297. [PubMed: 14501011]

39. Jung HI, Bowden SJ, Cooper A, Perham RN. Thermodynamic analysis of the binding of component enzymes in the assembly of the pyruvate dehydrogenase multienzyme complex of *Bacillus stearothermophilus*. Protein Sci 2002;11:1091–1100. [PubMed: 11967366]
40. Goncalves E, Kitas E, Seelig J. Structural and thermodynamic aspects of the interaction between heparan sulfate and analogues of melittin. Biochemistry 2006;45:3086–3094. [PubMed: 16503664]
41. Fath M, VanderNoot V, Kilpelainen I, Kinnunen T, Rauvala H, Linhardt RJ. Interaction of soluble and surface-bound heparin binding growth-associated molecule with heparin. FEBS Lett 1999;454:105–108. [PubMed: 10413105]
42. Rathore D, McCutchan TF, Garboczi DN, Toida T, Hernaiz MJ, LeBrun LA, Lang SC, Linhardt RJ. Direct measurement of the interactions of glycosaminoglycans and a heparin decasaccharide with the malaria circumsporozoite protein. Biochemistry 2001;40:11518–11524. [PubMed: 11560500]
43. McCornack MA, Cassidy CK, LiWang PJ. The binding surface and affinity of monomeric and dimeric chemokine macrophage inflammatory protein 1 beta for various glycosaminoglycan disaccharides. J Biol Chem 2003;278:1946–1956. [PubMed: 12411442]
44. Ucci JW, Kobayashi Y, Choi G, Alexandrescu AT, Cole JL. Mechanism of interaction of the double-stranded RNA (dsRNA) binding domain of protein kinase R with short dsRNA sequences. Biochemistry. 2007in press
45. Williamson MP, Suzuki Y, Bourne NT, Asakura T. Binding of amyloid beta-peptide to ganglioside micelles is dependent on histidine-13. Biochem J 2006;397:483–490. [PubMed: 16626304]
46. Wizemann H, Garbe JH, Friedrich MV, Timpl R, Sasaki T, Hohenester E. Distinct requirements for heparin and alpha-dystroglycan binding revealed by structure-based mutagenesis of the laminin alpha2 LG4-LG5 domain pair. J Mol Biol 2003;332:635–642. [PubMed: 12963372]
47. Wilkins DK, Grimshaw SB, Receveur V, Dobson CM, Jones JA, Smith LJ. Hydrodynamic radii of native and denatured proteins measured by pulse field gradient NMR techniques. Biochemistry 1999;38:16424–16431. [PubMed: 10600103]
48. Beckmann G, Hanke J, Bork P, Reich JG. Merging extracellular domains: fold prediction for laminin G-like and amino-terminal thrombospondin-like modules based on homology to pentraxins. J Mol Biol 1998;275:725–730. [PubMed: 9480764]
49. Denzer AJ, Schulthess T, Fauser C, Schumacher B, Kammerer RA, Engel J, Ruegg MA. Electron microscopic structure of agrin and mapping of its binding site in laminin-1. EMBO J 1998;17:335–343. [PubMed: 9430625]
50. Hohenester E, Tisi D, Talts JF, Timpl R. The crystal structure of a laminin G-like module reveals the molecular basis of alpha-dystroglycan binding to laminins, perlecan, and agrin. Mol Cell 1999;4:783–792. [PubMed: 10619025]
51. Stiegler AL, Burden SJ, Hubbard SR. Crystal structure of the agrin-responsive immunoglobulin-like domains 1 and 2 of the receptor tyrosine kinase MuSK. J Mol Biol 2006;364:424–433. [PubMed: 17011580]
52. Till JH, Becerra M, Watty A, Lu Y, Ma Y, Neubert TA, Burden SJ, Hubbard SR. Crystal structure of the MuSK tyrosine kinase: insights into receptor autoregulation. Structure 2002;10:1187–1196. [PubMed: 12220490]
53. Tisi D, Talts JF, Timpl R, Hohenester E. Structure of the C-terminal laminin G-like domain pair of the laminin alpha2 chain harbouring binding sites for alpha-dystroglycan and heparin. EMBO J 2000;19:1432–1440. [PubMed: 10747011]
54. Gesemann M, Denzer AJ, Ruegg MA. Acetylcholine receptor-aggregating activity of agrin isoforms and mapping of the active site. J Cell Biol 1995;128:625–636. [PubMed: 7860635]
55. Wallace BG. Regulation of agrin-induced acetylcholine receptor aggregation by Ca^{++} and phorbol ester. J Cell Biol 1988;107:267–278. [PubMed: 2839519]
56. Gee SH, Montanaro F, Lindenbaum MH, Carbonetto S. Dystroglycan-alpha, a dystrophin-associated glycoprotein, is a functional agrin receptor. Cell 1994;77:675–686. [PubMed: 8205617]
57. Scotton P, Bleckmann D, Stebler M, Sciandra F, Brancaccio A, Meier T, Stetefeld J, Ruegg MA. Activation of muscle-specific receptor tyrosine kinase and binding to dystroglycan is regulated by alternative mRNA splicing of agrin. J Biol Chem 2007;281:36835–36845. [PubMed: 17012237]
58. Hohenester E, Engel J. Domain structure and organisation in extracellular matrix proteins. Matrix Biol 2002;21:115–128. [PubMed: 11852228]

59. Cotman SL, Halfter W, Cole GJ. Agrin binds to beta-amyloid (Abeta), accelerates abeta fibril formation, and is localized to Abeta deposits in Alzheimer's disease brain. Mol Cell Neurosci 2000;15:183–198. [PubMed: 10673326]

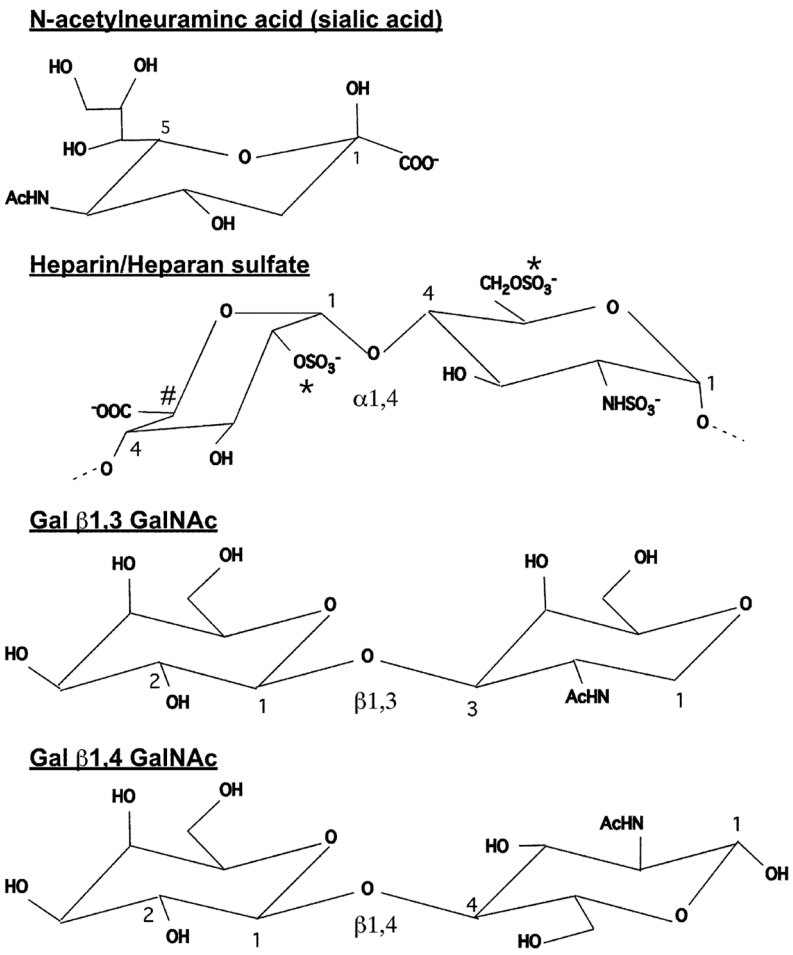

Figure 1.

Structures of the carbohydrates investigated in this study. The structure for heparin/heparan sulfate shows the most common [IdoA(2S)-GlcNS(6S)] disaccharide unit. The asterisks show positions where the substituent can be either a hydrogen (–H) or sulfate ($–SO_3^-$). The heparin polymer is more heavily modified and has more sulfate groups than heparan sulfate. The pound sign indicates that the carboxyl group on the 5-carbon can exist in multiple epimerization states.

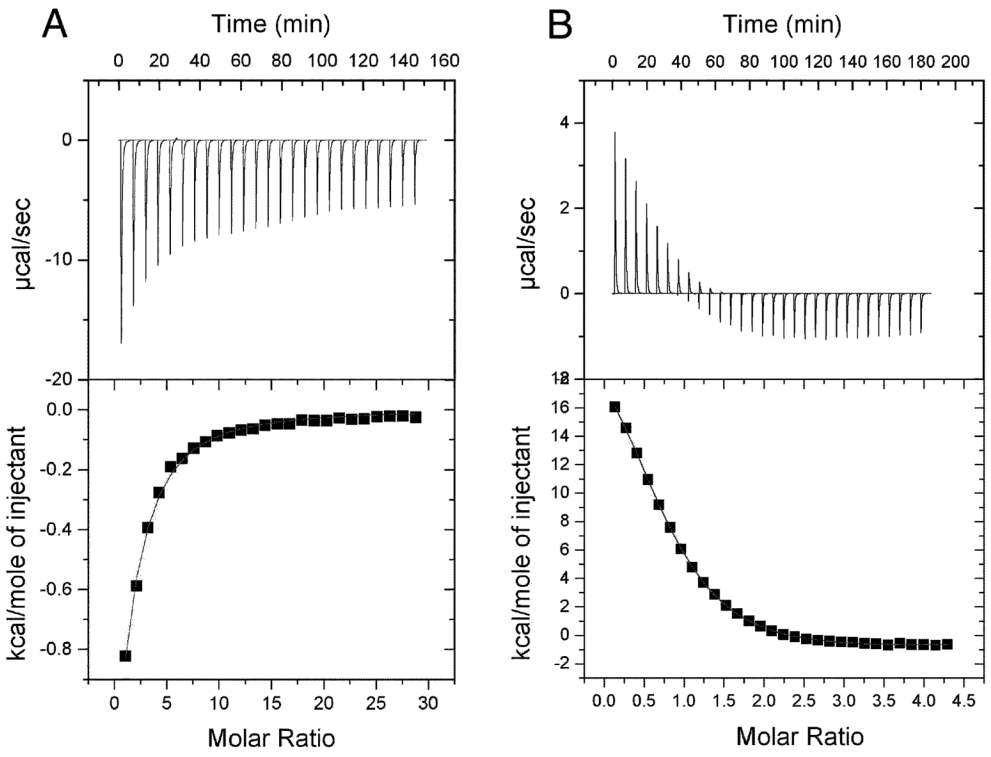

Figure 2.

Representative ITC data for binding of sialic acid (A) and heparin (B) to agrin-G3. The top panels show the raw ITC data, and the bottom panels show fits of the data after subtraction of background heats determined in ligand-to-buffer experiments. Thermodynamic parameters derived from the ITC data are given in Table 1.

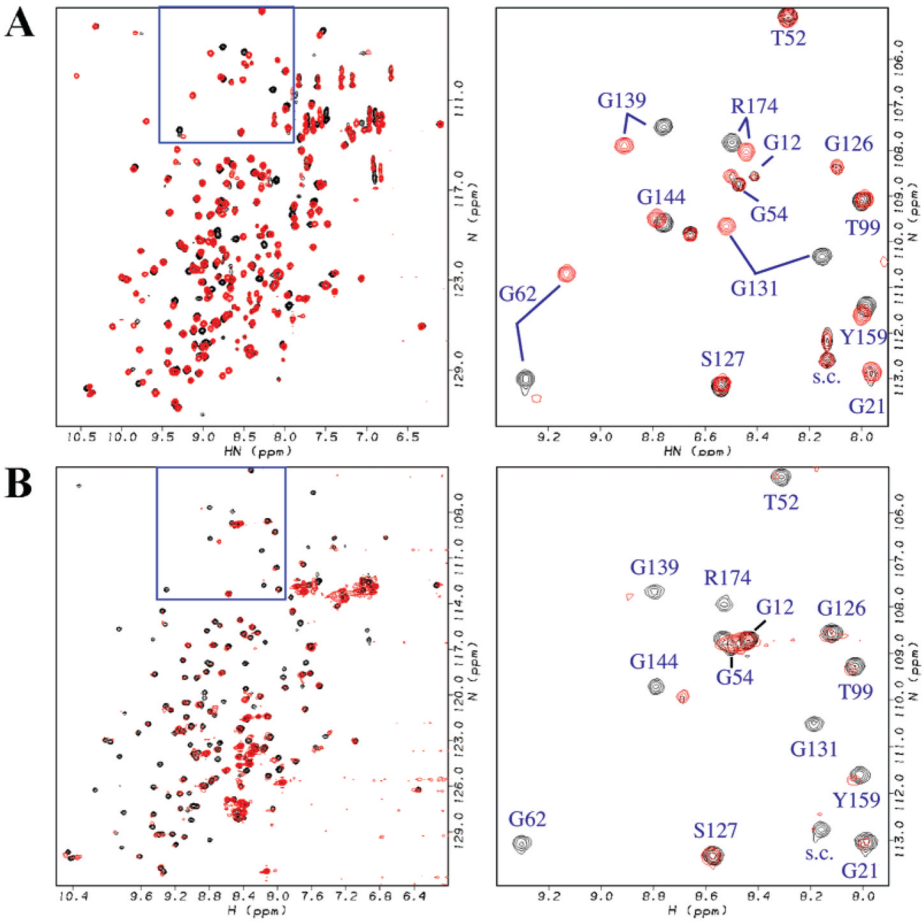

Figure 3.

Ligand-induced changes in $^{1}H–^{15}N$ HSQC spectra of agrin-G3. Superposition of spectra showing (A) 0.33 mM B0 alone and in the presence of 5 mM sialic acid and (B) 0.15 mM B0 alone and in the presence of ~2 mM heparin. Spectra of the free protein are shown in black; those with ligand are in red. The panels on the right are expansions of the regions shown in the blue boxes. Cross-peaks in the expansions are labeled according to residue position in the amino acid sequence. The cross-peak marked s.c. is from side-chain amide resonances of Gln117.

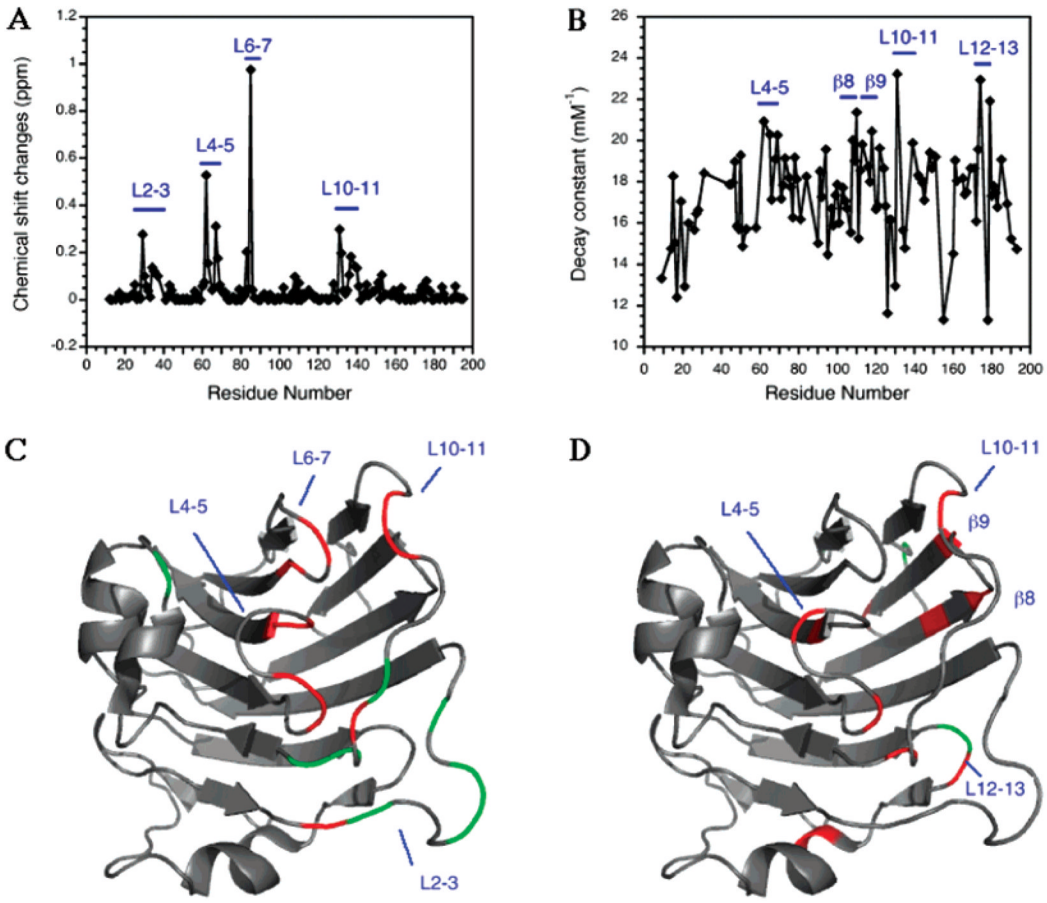

Figure 4.

Mapping of ligand-induced changes in $^{1}H–^{15}N$ HSQC spectra on the NMR structure of the agrin-G3 domain (8). (A) Weighted chemical shift changes accompanying sialic acid binding, calculated as $\Delta\delta_{av} = (\Delta\delta_H^2 + 0.1\Delta\delta_N^2)^{1/2}$. (B) Decay constants for NMR signals accompanying heparin binding, obtained using the equation $y = A \exp^{-k[\text{heparin}]} + C$, where k is an empirical decay constant and C is the baseline intensity at saturating heparin concentration (44). (C) Structural mapping of the largest chemical shift changes accompanying sialic acid binding: green, values above 0.10 ppm; red, values above 0.15 ppm. (D) Structural mapping of the largest decay constants for heparin-induced line broadening: green, values above 19.5 mM^{-1}; red, values above 20.0 mM^{-1}. Loops with residues that experience large NMR signal perturbations when ligands bind are designated according to the β-strands they connect. The L4–5, L6–7, and L10–11 loops contribute ligands to the Ca^{2+} ion bound by agrin-G3. The L2–3 loop bears the B8, B11, and B19 sequence inserts in the neural isoform of agrin and contributes to Ca^{2+} binding through a bridging water molecule (8).

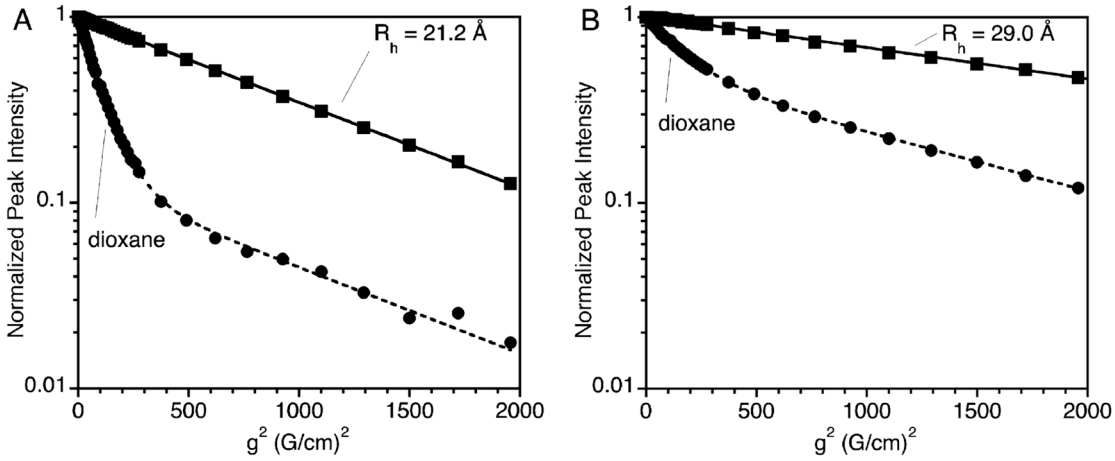

Figure 5.

PFG diffusion data for B0 alone (A) and in the presence of heparin (B). The *y*-axis data are on a logarithmic scale. Peak decays as a function of the square of gradient strength were fit to a single exponential for the protein (solid line) and to a double exponential (47) for the dioxane standard (dashed line).

Table 1

ITC Results for Binding of Ligands to the Agrin-G3 Domain[a]

ligand–agrin-G3 isoform	K_d (μM)	*n*	ΔG (kcal/mol)	ΔH (kcal/mol)	ΔS [cal/(mol•K)]
Ca^{2+}–B0	260 ± 8	1,23 ± 0.14	−4.88 ± 0.02	−8.0 ± 0.9	−10.5 ± 3.0
Ca^{2+}–B8	503 ± 25	1[b]	−4.49 ± 0.03	−7.2 ± 0.2	−9.1 ± 0.7
sialic acid–B0[c]	928 ± 84	1.05 ± 0.26	−4.13 ± 0.05	−3.9 ± 1.0	0.8 ± 3.4
sialic acid–B8[c]	1472 ± 80	0.68 ± 0.46	−3.86 ± 0.03	−9.3 ± 6.5	−18 ± 22
heparin–B0[d]	12.8 ± 0.6	0.78 ± 0.01	−6.66 ± 0.03	24.0 ± 0.5	103 ± 2
heparin–B8[d]	9.6 ± 0.4	0.82 ± 0.01	−6.83 ± 0.03	18.2 ± 0.3	84 ± 1
heparan sulfate–B0[d]	6.7 ± 0.6	0.25 ± 0.01	−7.04 ± 0.05	22.4 ± 1.3	99 ± 4
heparan sulfate–B8[d]	21.1 ± 6.5	0.15 ± 0.10	−6.36 ± 0.18	43.8 ± 33.0	170 ± 110

[a] All experiments were done at a temperature of 25 °C. Protein and ligand concentrations for the experiments are given in the ITC section of the Experimental Procedures.

[b] The stoichiometry was fixed to $n = 1$ since it is known that agrin-G3 binds one calcium ion (8,28). The parameters obtained in this fit with *n* as a free variable were $n = 0.33 \pm 1.51$, $K_d = 526 \pm 76$ μM, and $\Delta H = -22 \pm 10$.

[c] Experiments were done in the presence of a saturating concentration of 17 mM $CaCl_2$. Sialic acid does not bind the agrin-G3 domain in the absence of Ca2+.

[d] The experiments with heparin and heparan sulfate where done in the absence of Ca^{2+} with protein that was pretreated with EDTA.